Bacterial Nanocellulose-Reinforced Arabinoxylan Films

Jasna S. Stevanic,[1] Catherine Joly,[2] Kirsi S. Mikkonen,[3] Kari Pirkkalainen,[4] Ritva Serimaa,[4] Caroline Rémond,[2] Guillermo Toriz,[5] Paul Gatenholm,[5] Maija Tenkanen,[3] Lennart Salmén[1]

[1]*INNVENTIA AB, Fibre and Material Science, SE-114 86 Stockholm, Sweden*
[2]*UMR FARE 614 INRA, University of Reims, Champagne Ardenne, 51688 Reims, France*
[3]*Department of Food and Environmental Sciences, University of Helsinki, FIN-00014 Helsinki, Finland*
[4]*Department of Physics, Materials Physics, University of Helsinki, FIN-00014 Helsinki, Finland*
[5]*Department of Chemical and Biological Engineering, Wallenberg Wood Science Center, Chalmers University of Technology, SE-412 96 Gothenburg, Sweden*

Received 27 October 2010; accepted 24 January 2011
DOI 10.1002/app.34217
Published online 20 May 2011 in Wiley Online Library (wileyonlinelibrary.com).

ABSTRACT: There is an increasing interest in substituting today's films for food packaging applications with films based on renewable resources. For this purpose, rye arabinoxylans, unmodified and enzymatically debranched, were studied for the preparation of neat films and composite films reinforced with bacterial cellulose (BC). Mixing in a homogenizer produced optically transparent, uniform films. Physical and mechanical characteristics of such films are here reported. Debranching of the arabinoxylan caused an increase in its crystallinity of 20%. Debranching as well as reinforcement with BC resulted in a decrease of the moisture sorption of the films. The debranching also resulted in a reduced breaking strain while the reinforcement with BC increased stiffness and strength of the films. © 2011 Wiley Periodicals, Inc. J Appl Polym Sci 122: 1030–1039, 2011

Key words: arabinoxylan; bacterial cellulose; composite film; moisture; strength properties

INTRODUCTION

Production of environmentally friendly packaging materials, based on renewable polymers, is increasingly demanded. Films made of polar plant-derived nonfood polysaccharides, such as hemicelluloses (xylans and glucomannans) and cellulose, may provide a potential alternative for future-biobased packaging materials. These polymers are hydrophilic and as such show good barrier properties against oils and fats, but they are not efficient as moisture and water vapor barriers.[1] This property needs to be improved to be able to use hemicelluloses films, particularly for food-packaging purposes. Hemicelluloses, particularly xylans, make a dense network showing good oxygen-barrier properties.[2–4] The mechanical strength of hemicellulose-based films does however vary considerably. One possibility to enhance the performance of hemicellulose films is by reinforcing them with bacterial cellulose (BC) thus initiating this study.

Arabinoxylans are a group of structural polysaccharides that can be found in almost all annual plants, and many woody plants, such as softwoods.[5,6] The function of arabinoxylans is to make up the matrix in the plant cell wall and also to integrate with the cellulose fibrils. The chemical structure of arabinoxylans varies significantly depending on their source. The backbone of arabinoxylans is built up of (1 → 4)-linked β-D-xylopyranosyl units, which are further substituted with varying degrees by α-L-arabinofuranosyl groups.[7,8] Other substituents found in arabinoxylans are α-D-glucopyranosyl uronic acid (or its 4-*O*-methyl ether), D-xylopyranosyl, acetyl, and feruloyl groups.[7,8] Cereal cell walls, such as from barley, husk, oat, and rye, are rich in arabinoxylans and therefore an attractive source, because they represent nonfood fractions and a potential agricultural waste. In rye (*Secale cereale*) endosperm arabinoxylan, the β-D-xylopyranosyl units are both mono- and disubstituted by (1 → 2)- and (1 → 3)-linked α-L-arabinofuranosyl units (Fig. 1). The ratio of mono and disubstituted xylopyranosyl residues is 2 : 1, and the average arabinose to xylose (Ara/Xyl) ratio is between 0.50 and 1.00.[3]

BC is produced by the cultivation of *Acetobacter xylinum* in an aqueous medium-containing sugar source, such as glucose. This BC has the same chemical composition as plant cellulose, that is, long linear molecules composed of (1 → 4)-linked β-D-glucopyranosyl units assembled into hierarchical structures of microfibrils possessing excellent strength and stiffness.[9] The size of such BC is in nanoscale, having an average width of 10 nm and a length of more than 2 μm.[10] For that reason, this BC was used as a nanocellulosic model component in this study.

Correspondence to: L. Salmén (lennart.salmen@innventia.com).

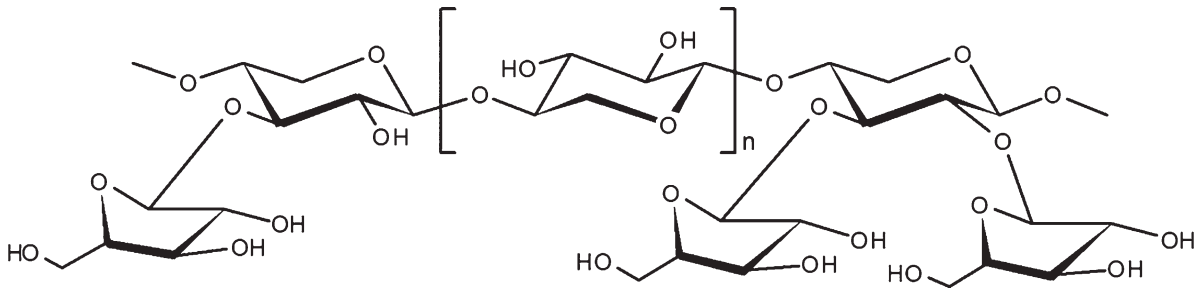

Figure 1 Chemical structure of rye arabinoxylan.

The aim of this study was to investigate the morphology, physical, and mechanical properties of different composite films made from native rye arabinoxylan (rAX) and enzymatically debranched rye arabinoxylan (rDAX) (D denoting debranched) together with BC at low to moderate degrees of reinforcement in [5 and 15% of BC (w/w)].

MATERIALS AND METHODS

Preparation of rAX solution

A high-molecular weight rAX (lot 20601a) was used (Megazyme International Ireland); molar mass 289,300 g/mol.[11] The arabinose/xylose (Ara/Xyl) ratio of the rAX was 0.50. An aqueous arabinoxylan solution was prepared by dissolving the rAX flour (prewetted with 95% C_2H_5OH) in deionized water, heating it at 100°C under magnetic stirring for 10 min. The solution was allowed to cool down under magnetic stirring to room temperature, and its concentration was adjusted to 1% (w/v).

Enzymatic modification of rAX

Debranching of rAX was carried out by a treatment with endoxylanase-free α-arabinofuranosidase, which was kindly obtained from Novozymes (Bagsvaerd, Denmark). The α-arabinofuranosidase activity of the enzyme preparation was determined according to Poutanen.[12] The enzyme efficiently liberates the α-L-arabinofuranosyl residues from the monosubstituted β-D-xylopyranosyl units.[3]

rAX was dissolved in water as described earlier, whereas the concentration of the rAX solution was adjusted to 2% (w/v). An equal volume of the rAX solution and 50 m*M* sodium acetate buffer, pH 5.0 containing α-arabinofuranosidase was mixed and incubated for 24 h at 40°C with stirring. The enzyme dosages used was 5000 nkat/g of rAX. After incubation, the enzyme action was terminated by keeping the solution in a boiling water bath for 15 min. A small sample (100 μL) was taken aside for further analysis of the released arabinose, and the arabinoxylan solution was dialyzed for 48 h (MWCO 12–14,000 Da) against water to remove buffer ions and released arabinose. The amount of released arabinose was measured with a lactose/galactose assay kit according to manufacturer's instructions (K-LACGAR, Megazyme). The sample was centrifuged for 10 min at 10,000 rpm before analysis to remove nonsoluble material. According to the analysis, 68% of the total α-L-arabinofuranosyl units were removed, and the resulting Ara/Xyl ratio of the rDAX was 0.16. The rDAX sample was kept as a water suspension before its use in film preparation.

Biosynthesis of BC

A static cultivation of *Acetobacter xylinum*, subspecie BPR2001, in a fructose/corn steep liquor medium at 30°C[13] was used for the production of bacterial cellulose (BC). The cultivation time was 2 weeks. The produced cellulose pellicles were first treated in 1*M* NaOH at 80°C for 1 h and then in deionized water to remove the bacteria and to exchange the remaining media. The washed cellulose network was disintegrated in an ordinary laboratory blender, and its concentration was adjusted to 1% (w/v).[14]

Preparation of r(D)AX, r(D)AX : 5BC, and r(D)AX : 15BC films

Two series of films were prepared by mixing the BC dispersion with the arabinoxylan solutions in different proportions with the arabinoxylan/BC ratio of 100/0, 95/5, and 85/15. The first series of rAX films was made using arabinoxylan with an Ara/Xyl ratio of 0.50 (rAX, rAX : 5BC, and rAX : 15BC), while the second series was prepared from arabinoxylan with an Ara/Xyl ratio of 0.16 (rDAX, rDAX : 5BC, rDAX : 15BC). A list of the films with their codes and descriptions is given in Table I.

All the solutions and mixtures (totally six solutions/mixtures) were adjusted to a volume of 210 mL with deionized H_2O. No external plasticizer was added. The mixtures were then homogenized in a high-pressure microfluidizer (Microfluidizer M-110EH, Microfluidics Corp., Newton, MA) with an operating pressure of 1650 bar. The mixtures

TABLE I
Codes and Descriptions of Arabinoxylan and Bacterial Cellulose Composite Films Showing Mixing Proportions, Description of Mixing Procedure, and Film Characteristics

Code	Description of film	Description of mixing: amount, mass concentration, and volume of the material
rAX	100% rAX	1 g, 1%, 100 ml rAX
rAX : 5BC	95% rAX + 5% BC	1 g, 1%, 100 ml rAX + 0.053 g, 1%, 5.3 ml BC
rAX : 15BC	85% rAX + 15% BC	1 g, 1%, 100 ml rAX + 0.177 g, 1%, 17.7 ml BC
rDAX	100% debranched rAX	1 g, 0.67%, 149.3 ml rDAX
rDAX : 5BC	95% debranched rAX + 5% BC	1 g, 0.67%, 149.3 ml rDAX + 0.053 g, 1%, 5.3 ml BC
rDAX : 15BC	85% debranched rAX + 15% BC	1 g, 0.67%, 149.3 ml rDAX + 0.177 g, 1%, 17.7 ml BC

were passed through two Z-shaped chambers connected in series with a diameter of 200 μm and 100 μm, respectively. This homogenization procedure was repeated three times, in total. The resulting dispersions were exposed to vacuum under magnetic stirring for 2 h to remove air bubbles. The homogenized dispersions were then casted into either teflon evaporating plates (Ø10.2 and Ø6.5 cm) for studies of physical properties (thickness ~ 30 μm) or polystyrene petri dishes (Ø9.4 cm) for studies of mechanical properties (thickness ~ 20 μm). These were left to evaporate at 24°C and 28% relative humidity (RH) for 48 h.

Scanning electron microscopy analysis

SEM images of films, fractured in tensile mode at 50% RH and 30°C, were collected with a LEO ULTRA 55 FEG SEM (LEO electron microscopy LTD, Cambridge, UK) equipped with a field emission gun and a secondary electron detector. Acceleration voltage was set to 5kV. Before the SEM analysis, the films were glued to aluminum specimen mount with a colloidal silver liquid and sputter coated with a thin layer of gold.

Wide-angle X-ray scattering

Wide-angle X-ray scattering measurements were carried out in the perpendicular transmission geometry using Cu $K\alpha_1$ radiation. A set up with a Rigaku rotating anode (fine focus) X-ray tube (Rigaku Corp., Tokyo, Japan) and a MAR345 image plate detector (Rayonix, Evanston, IL) was used. The beam was monochromated and focused on the detector with a bent Si(111) crystal and a totally reflecting mirror.

The recorded two-dimensional diffraction patterns were radially averaged to one-dimensional diffraction intensity profiles. The diffraction intensities were corrected to take into account of the attenuation of radiation inside the sample and the differences in diffracted ray paths due to the flat detector. The diffraction patterns of all the samples were measured at ambient room conditions of 23°C and 20% RH. Five replicates from each film type were tested.

The diffraction intensities are plotted as a function of scattering angle. The scattering angles are given in 2θ, which is twice the value of the Bragg angle in Bragg's law

$$\lambda = 2d_{hkl}\sin\left(\theta\left[^{\circ}\right]\right) \quad (1)$$

or in wavelength-invariant form

$$q = \frac{2\pi}{d_{hkl}} = \frac{4\pi\sin(\theta)}{\lambda}\left[\frac{1}{\mathrm{A}}\right] \quad (2)$$

where λ is the wavelength of the incident radiation, and d_{hkl} is the distance of the planes given by Miller indices *hkl*.

The diffraction intensities were also used to evaluate the relative amount of crystalline and amorphous regions of xylan present in the samples. The 100% crystalline xylan diffraction pattern was calculated using the known crystal structure and atomic coordinates of xylan dihydrate.[15] The positions, intensities, and widths of all the reflections of xylan dihydrate in the angular range of 5°–60° were calculated using PowderCell 2.4 computer software.[16] The calculated diffraction pattern was then compared to the measured intensity profiles, and the lattice parameters, *a* and *c*, of the hexagonal crystal structure were refined until the fit with measured data was best fitted.

Dielectric analysis

For dielectric testing, a TA Instruments Dielectric Analyzer (DEA 2970, TA instruments, USA) was used in multifrequency mode to determine the glass transition temperature, (T_g), in the dry state from the maximum of tan δ. The samples were cut into small discs (Ø5 mm), which were dried in the analyzer for 2 h at 80°C without any seal contact pressure between the electrodes and under dry nitrogen (N_2) flux. Then, a second run was applied from room temperature until 150°C at 3°/min under dry N_2

flux. This procedure was adopted to obtain a constant measure of tan δ. A constant force of 50*N* was applied at 1 Hz during the experiment. Five replicates from each film type were tested.

Water sorption isotherms

An IGA sorption microbalance (IGA0.02 Hiden Isochema, UK) was used to collect water sorption isotherms at 20°C. The sensors, for RH control, were calibrated with commercial saturated salt at 20°C. Film pieces were mounted in the pan of the balance and dried at 40°C until equilibrium under dry N_2 flux. The dry weight was then recorded at a temperature of 20°C. Two replicates from each film type were tested. The moisture uptake was expressed according to eq. (3):

$$\text{Moisture uptake} = 100\frac{W_{\text{moist}} - W_{\text{dry}}}{W_{\text{dry}}} \qquad (3)$$

where W_{moist} is the sample weight equilibrated at the chosen RH and W_{dry} is the weight of the dry sample.

Tensile testing

Mechanical testing was carried out on a dynamic mechanical analyzer Perkin–Elmer DMA 7e (PerkinElmer Corp., Norwalk, CT) operating in tension mode. Films of 20 μm thickness of the r(D)AX, r(D)AX : 5BC, and r(D)AX : 15BC with the dimensions of 5 × 20 mm (width-length) were used for stress–strain tests at 50% RH and 30°C. The applied loading rate was 500 mN/min. Ten replicates from each film type were tested. The Young's modulus (E) was taken as the initial slope of the linear part of the stress–strain curve. The stress at break (σ_b) and strain at break (ε_b) were evaluated based on the initial sample dimensions.

Dynamic mechanical analysis

Dynamic mechanical testing was carried out using a Perkin–Elmer DMA 7e (PerkinElmer Corp.). Films of 20 μm thickness of r(D)AX, r(D)AX : 5BC, and r(D)AX : 15BC with the dimensions of 2 × 15 mm (width-length) were first conditioned at 0% RH and then scanned in a range of 1–90% RH at a speed of 1% RH/5 min at a temperature of 30°C. The desired relative humidities were achieved by mixing dry air and water-saturated air using a Wetsys humidity generator (Setaram Instrumentation, Caluire, France). The static load was adjusted to be equal to 120% of the dynamic load, the amplitude was set to be constant at 8 μm, and a frequency of 1 Hz was applied. Three replicates from each film type were tested. The storage modulus (E') and the loss tangent (tan δ) were recorded using a Pyris DMA 28 software (PerkinElmer Corp.).

RESULTS AND DISCUSSION

Both the rAX and rDAX were able to form cohesive films without the use of any added plasticizer. In the case of the composite films, cohesive transparent films were also produced.

Figure 2 shows SEM micrographs of the fracture surfaces of representative films. The micrographs of the pure rAX and rDAX films show quite homogenous structures where the debranched arabinoxylan formed smaller aggregated particles than the unmodified arabinoxylan. In the composite films, the fibrous phase of reinforcing BC was more aggregated in the rAX : 15BC film than in the rDAX : 15BC. This could be explained by an improved interaction between the arabinoxylan and BC occurring when the arabinose (Ara) units were removed.

Film morphology

Figure 3 shows the X-ray diffraction patterns of the different films. For the untreated rAX, only a wide halolike feature centered at about 20° 2θ was shown, and no definite diffraction maxima in the measured angular range. The halo can be interpreted as diffraction from very short range electron density correlations, and it is safe to say that there was no long range order of atomic arrangement of any kind in this sample. Therefore, the diffraction pattern of rAX was used as an amorphous background for crystallinity analysis of the other samples of this study. In other words, the calculated xylan crystallinity values are given relative to rAX, and, for convenience, the crystallinity of rAX was assumed to be zero.

The diffraction intensities measured from the rAX : 5BC and rAX : 15BC films were similar to the one from the untreated rAX, with the difference of the component of diffraction from the BC. When the component of BC was subtracted, the crystallinity of the xylan in rAX : 5BC and rAX : 15BC films was calculated to be near zero 0% ± 2%.

The diffraction intensity of the film made from the debranched arabinoxylan (rDAX) showed several definite diffraction maxima in addition to the halolike background. Thus, the xylan in this film was semicrystalline 20% ± 3%, that is, there were regions of xylan crystallites surrounded by amorphous regions. The crystallite size of single crystallites was calculated from the reflections from the (110) planes, which showed the highest intensities, and by using the widths of the diffraction maxima and the Scherrer equation.[17] The average size of the single xylan

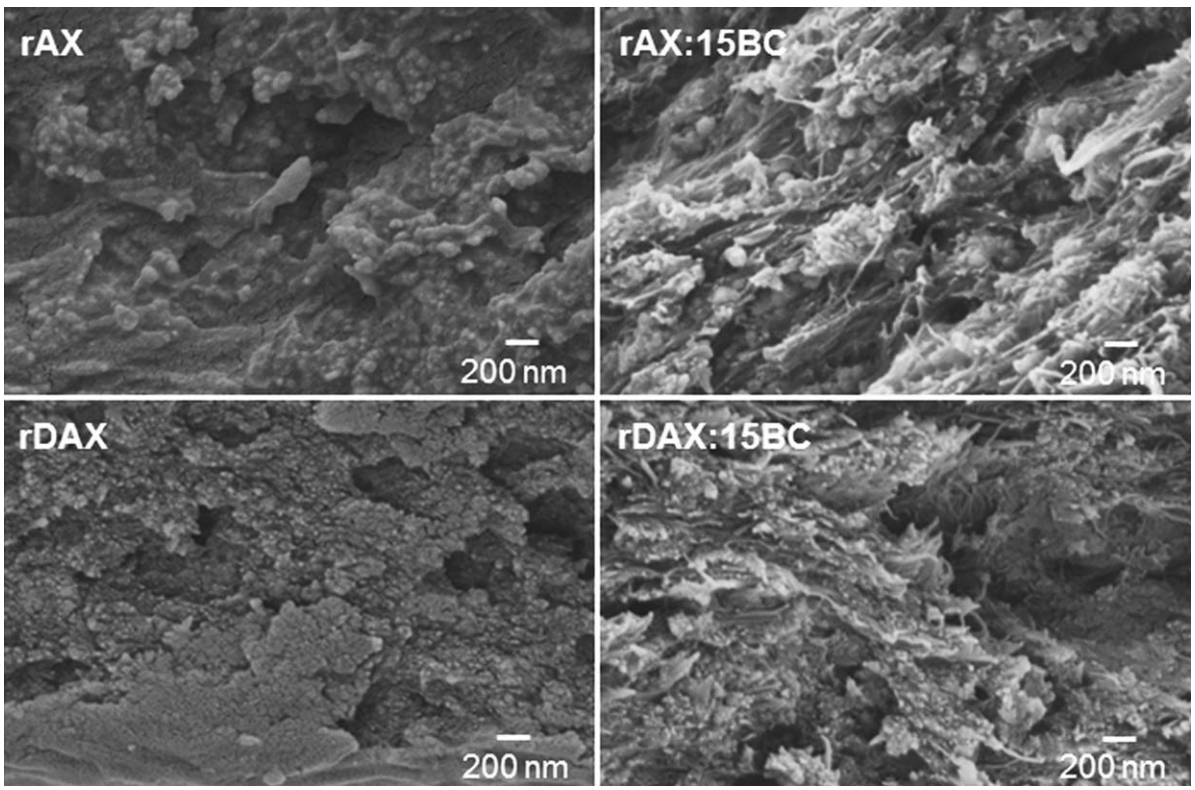

Figure 2 SEM micrographs of fracture surfaces of rye arabinoxylan films, unmodified rAX, and enzymatically modified rDAX, and corresponding composite films with 15% (w/w) bacterial cellulose. The scale bar is 200 nm.

crystallites was determined to be 6.3 ± 0.3 nm. The intensity patterns showed that the crystallites had no preferred orientation in the plane of the film.

The diffraction intensities measured from the rDAX : 5BC and rDAX : 15BC films were similar to the one from the debranched arabinoxylan (rDAX).

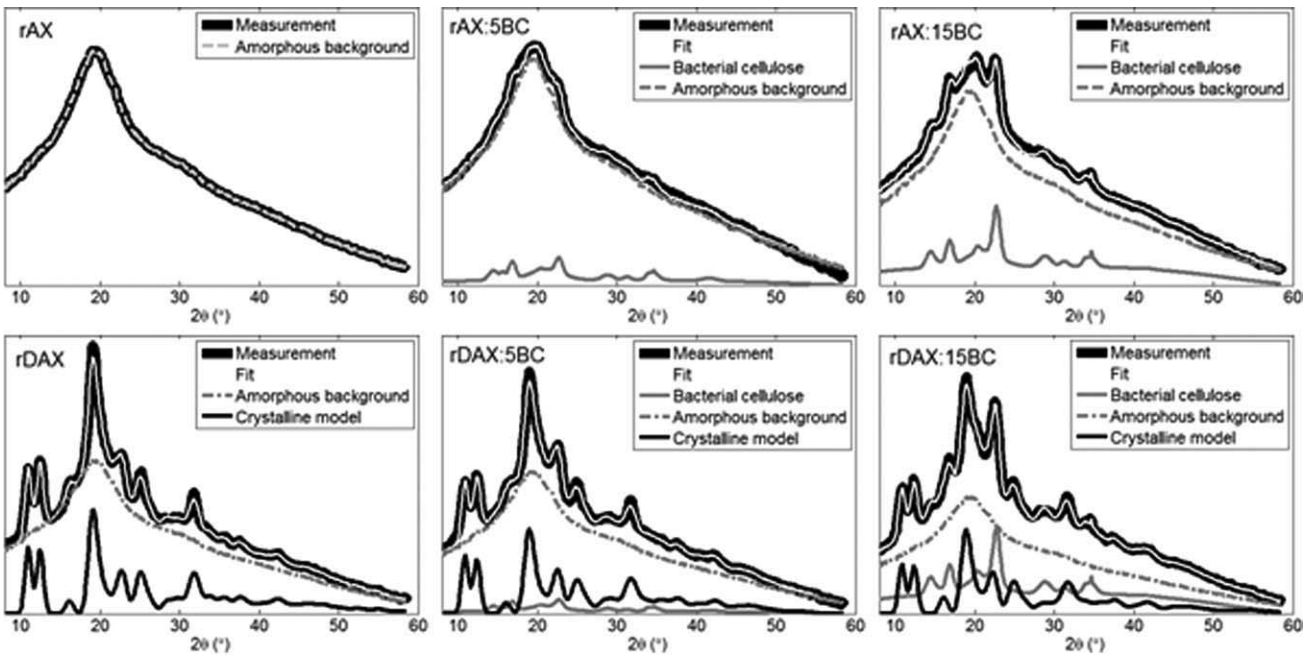

Figure 3 Wide angle X-ray diffraction intensity profiles of the studied films indicating the fitted diffraction components; rAX, rAX:5BC, rAX:15BC, rDAX, rDAX:5BC, and rDAX:15BC. The diffraction pattern of rAX was used as amorphous background for the crystallinity calculations. The fit resulting from all diffraction components is drawn as a solid white line.

TABLE II
Average Values of Glass Transition Temperature (T_g) at 1 Hz, for the Xylan and Composite Films Studied

Code	T_g (°C)
rAX	135 (4)
rAX : 5BC	139 (5)
rAX : 15BC	144 (10)
rDAX	141 (6)
rDAX : 5BC	129 (4)
rDAX : 15BC	135 (1)

Values in brackets are standard deviations.

When the component of BC was subtracted, the crystallinity of xylan was calculated to be the same as for the pure rDAX; 19% ± 3% for rDAX : 5BC and 21% ± 3% for rDAX : 15BC.

According to the refinement of the lattice parameters, the unit cell of xylan in the rDAX films was somewhat compacted perpendicular to the chain axis (lattice parameters $a = b = 9.33$ Å) when compared with the xylan dihydrate model ($a = b = 9.64$ Å). The lattice parameter c, which corresponds to the length of unit cell parallel to chain axis, was the same in the rDAX films as in the model within the uncertainty of the analysis.

Glass transition temperature (T_g)

The glass transition temperatures of the dry samples are given in Table II. The T_g obtained for neat films (rAX and rDAX) is nearly the same, but the standard deviation was much higher for the rDAX sample indicating more variable samples. The impact of the crystallization for the rDAX sample (20%) may have lead to a decrease in the macromolecular mobility indicated by the slight higher T_g. The presence of BC seems to increase the T_g, thus decreasing the mobility for the filled sample for the unmodified xylan. But, here again, the standard deviations are high. For the modified xylans, the T_g was nearly constant whatever the content of the BC. A slight decrease could be noticed between the pure debranched xylan and composites, but the standard deviations were too high to be able to draw a clear conclusion. At 95% confidentiality, only the T_g of the rDAX : 5BC film was significantly different from all the other films investigated (t-test).

Water sorption isotherms

The moisture sorption isotherm of all films made of rAX and rDAX both as pure films and with reinforced BC displayed a sigmoidal shape (Fig. 4). At low RH, the rAX and rDAX films absorbed similar amounts of moisture, whereas at increasing RH up to 80% led to a higher moisture uptake for the rAX film (larger content of arabinosyl groups) [Fig. 4(a)]. The lower moisture uptake for the enzymatically debranched arabinoxylan film could probably be related to, on one hand, the presence of unsubstituted regions in the xylan chains increasing interchain aggregation via hydrogen bonds preventing parts of the rDAX to absorb moisture, and, on the other hand, to a lowering of the available hydroxyl groups due to the removal of arabinose groups. This is in agreement with the X-ray measurements indicating xylan crystallization for the rDAX when compared with the amorphous rAX. Similar observations

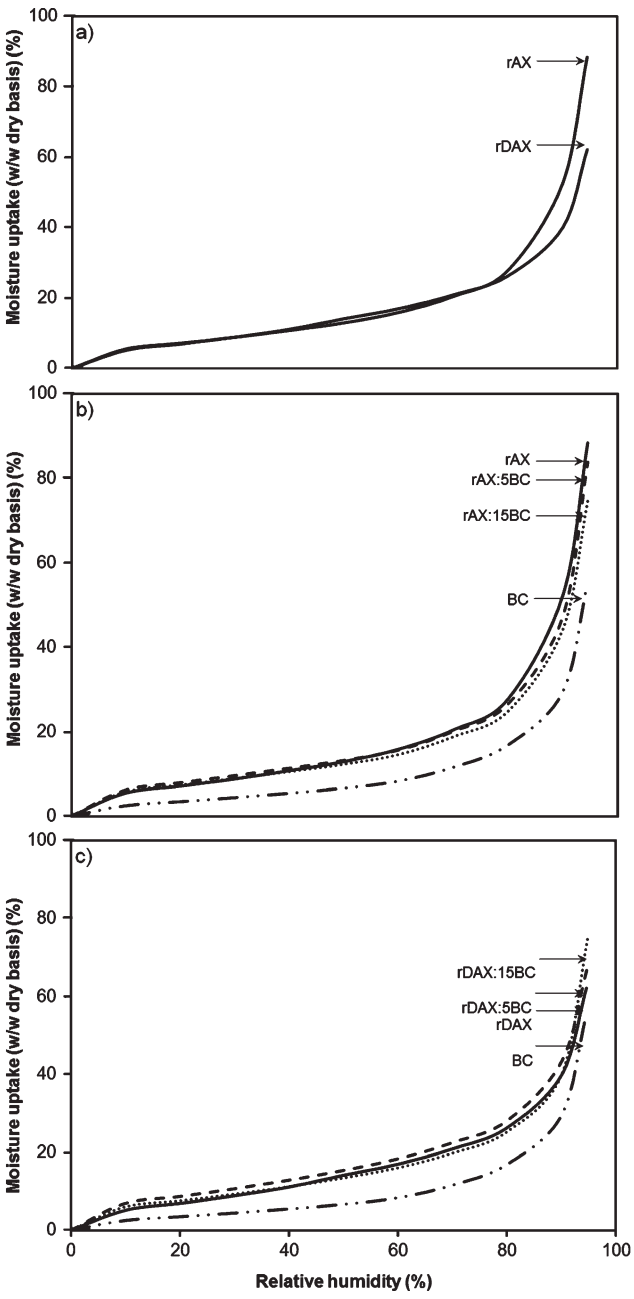

Figure 4 Water sorption isotherms as a function of relative humidity at 20°C for (a) neat films, (b) neat and composite films, rAX, and (c) neat and composite films, rDAX.

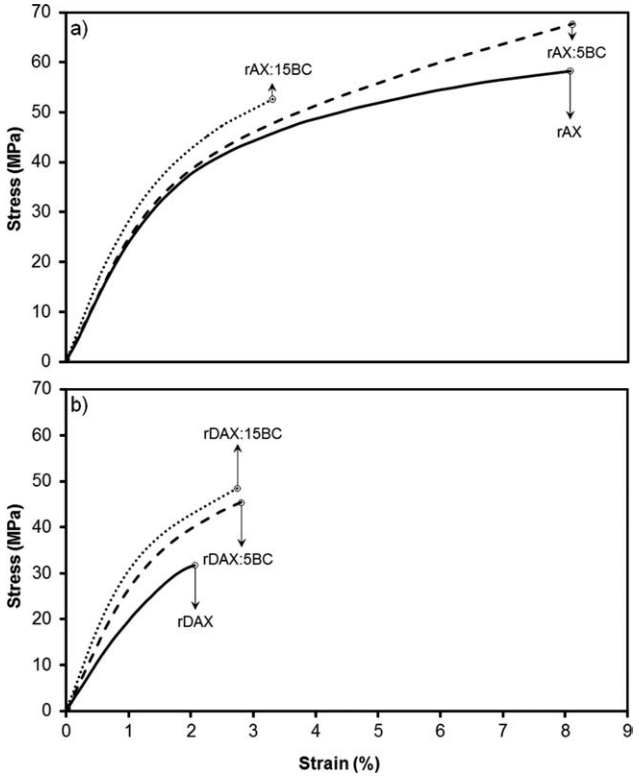

Figure 5 Stress–strain curves of composite films recorded at 50% RH, 30°C; (a) rAX and (b) rDAX.

have been made for wheat flour arabinoxylans[18] and for enzymatically tailored rAXs[3] where X-ray showed the development of a crystalline network.

Pure BC sheets showed a low moisture uptake reflecting its high crystallinity [Fig. 4(b,c)]. For the rAX composite films, the moisture uptake profiles were quite similar to that of the pure rAX films [Fig. 4(b)]. At high-relative humidities, the incorporation of BC decreased slightly the moisture uptake due to the lower moisture uptake of BC. Compared to the theoretical moisture sorption isotherm, calculated as the summation of the BC and rAX isotherms (data not shown), a somewhat higher sorption than what was experimentally found was predicted. This difference could be attributed to interactions between BC and xylan, taking the available water sorption sites, as no increased crystallinity of xylan by adding BC was noticed; X-ray data.

For the debranched xylan composites, the moisture uptake increased to some minor extent with the addition of BC [Fig. 4(c)]. This behavior was surprising but occurred only at very high RH. As the crystallinity remained unchanged with the addition of BC, the water sorption behavior of these rDAX films can be assumed as very similar to those observed for the rAX composites. This means that the addition of the BC only slightly affects the moisture uptake, whereas the removal of arabinose units from arabinoxylan reduced the moisture uptake more significantly. This reduction of the moisture uptake for rDAX occurred at high relative humidities, whereas at lower relative humidities, the moisture uptake remained the same.

Mechanical properties

Figure 5 shows average stress–strain curves of the different films tested at 50% RH, 30°C. The film of untreated rAX seems to be stiff, strong, and ductile (see Table III), while the enzymatically modified arabinoxylan (rDAX) appears as rather stiff, less strong, and more brittle. The increase in brittleness, when removing Ara groups as for the rDAX film, can be explained by the increased crystallinity (20%). The simultaneous decrease also in strength and stiffness may be a result of microscopic phase separation occurring as a result of the agglomeration (see Fig. 2). Similar results comparing the strength and elongation of rAX (Ara/Xyl ratio 0.50) and rDAX (Ara/Xyl ratio 0.20) films were recently reported by Höije et al.[3]

With the addition of BC to arabinoxylan, the composite films seemed to be stiffer; the higher the amount of BC the higher the stiffness of the films. Also, with one exception (i.e., rAX : 15BC), the strength and elongation of the composite films were improved. Surprisingly, when increasing the amount of the BC to 15% (w/w) for the unmodified arabinoxylan (rAX), a substantial decrease in the stress at break, σ_b, and the strain at break, ε_b, was noted. This deviation in the reinforcement effect for the rAX : 15BC film could probably be related to an agglomeration of BC occurring due to the low interacting with the highly substituted rAX as seen from the SEM micrographs in Figure 2. The stress–strain levels are though in line with similar data of high-BC reinforcement of glucuronoxylan films, alkali extracted from aspen wood chips.[10]

In general, debranching decreased the strength and elongation and improved the stiffness of corresponding films, both the neat and the composite

TABLE III
Average Values of Young's Modulus (E), Stress at Break (σ_b), and Strain at Break (ε_b) for Xylan Composite Films in Tensile Testing at 50% RH, 30°C

Code	Young's modulus, E (GPa)	Stress at break, σ_b (MPa)	Strain at break, ε_b (%)
rAX	2.5 ± 0.4	58 (11)	8.1 (3.3)
rAX : 5BC	2.7 ± 0.3	68 (11)	8.1 (3.1)
rAX : 15BC	3.2 ± 0.5	53 (7)	3.3 (0.6)
rDAX	2.2 ± 0.2	32 (3)	2.1 (0.3)
rDAX : 5BC	3.1 ± 0.4	46 (5)	2.8 (1.0)
rDAX : 15BC	3.7 ± 0.5	49 (8)	2.8 (1.3)

Values in brackets are standard deviations.

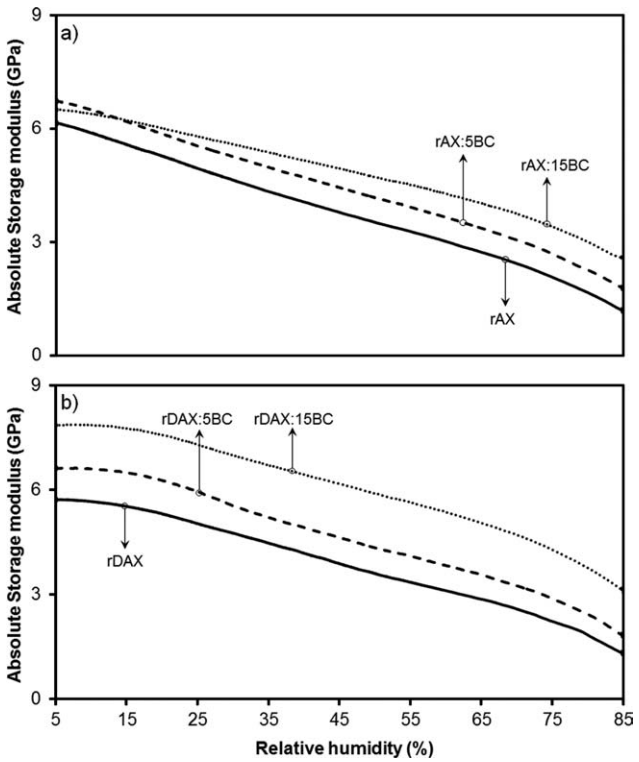

Figure 6 Storage modulus of composite films as a function of relative humidity; (a) rAX and (b) rDAX.

films (see Table III). An exception was a decreased stiffness (lowering of the Young's modulus value from 2.5 GPa to 2.2 GPa) for the pure rDAX film when compared with the rAX film. The lower the Young's modulus for the rDAX film can be related to its morphology, where small defects created by agglomeration due to lower solubility, which may result in a weaker film. This explanation was supported by the SEM micrograph of the rDAX film (Fig. 2), which displays a lot of small granules in this film.

The moisture effects on film stiffness are shown in Figure 6. With increasing amounts of BC, the films increased in stiffness. The increased crystallization occurring after debranching made the rDAX film slightly stiffer when compared with the rAX film. All the composite films made from the debranched xylan were stiffer than their corresponding films made from unmodified xylan. The rDAX : 15BC film appeared as the stiffest and the rAX film as the least stiff. The degree of substitution of a xylan molecule determines its ability to bond to cellulose. The higher the degree of substitution of side chains the lower is its bonding ability to cellulose, while molecules with fewer side chains binds more tightly to cellulose.[7] This fact may explain the higher stiffness for the composite films made with modified arabinoxylan, rDAX, having fewer Ara units.

In Figure 7, the relative moduli are compared for the rAX and the rDAX films, respectively. Moisture, clearly, acts as a plasticizer for the polysaccharides, as expected. The films made from the pure rAX as well as its composite films (i.e., rAX : 5BC and rAX : 15BC) showed a slightly higher degree of softening when compared with the corresponding films made from debranched arabinoxylan (i.e., rDAX, rDAX : 5BC, and rDAX : 15BC).

The higher the amount of BC, the lower was the degree of softening. This effect was mainly attributed to the reinforcing effect of the BC and its high stiffness, The difference between the two types of xylan should be related to the degree of substitution, which determines the degree of solubility of xylans by creating more free volume of the polymer molecule; the higher the degree of the substitution the higher the water solubility.[3,7] It was found that substitution of a xylan backbone increases its solubility, mainly by preventing effects of intermolecular hydrogen bonding.[8,19] When the arabinose side units are removed crystallization occurs, due to an increased ability of the unsubstituted regions of the backbone to form stable insoluble interchain aggregates. Previous studies have shown that only the backbone residues of different xylans take part in the crystallization[20] and that xylan chains show an ability to associate with each other and crystallize when the arabinose substituents are removed.[3,21–23]

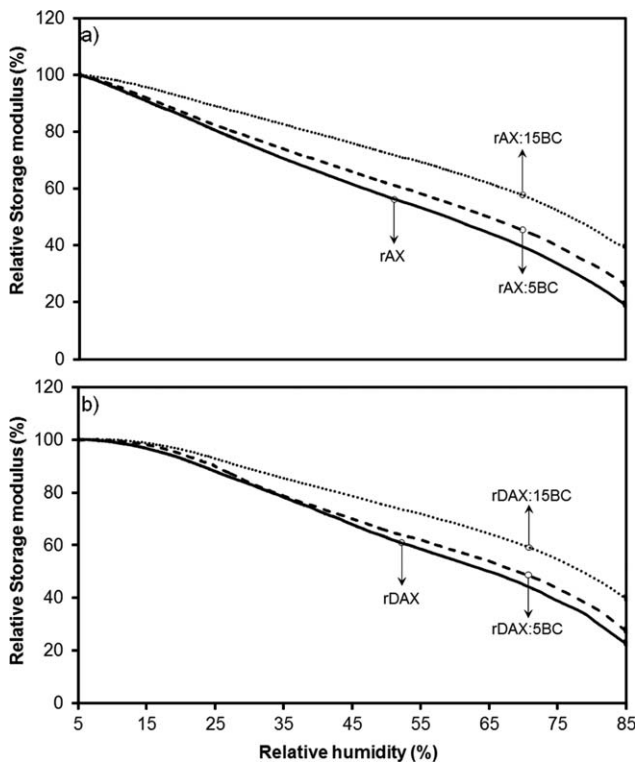

Figure 7 Relative storage modulus of composite films as a function of relative humidity, showing their softening ability; (a) rAX and (b) rDAX.

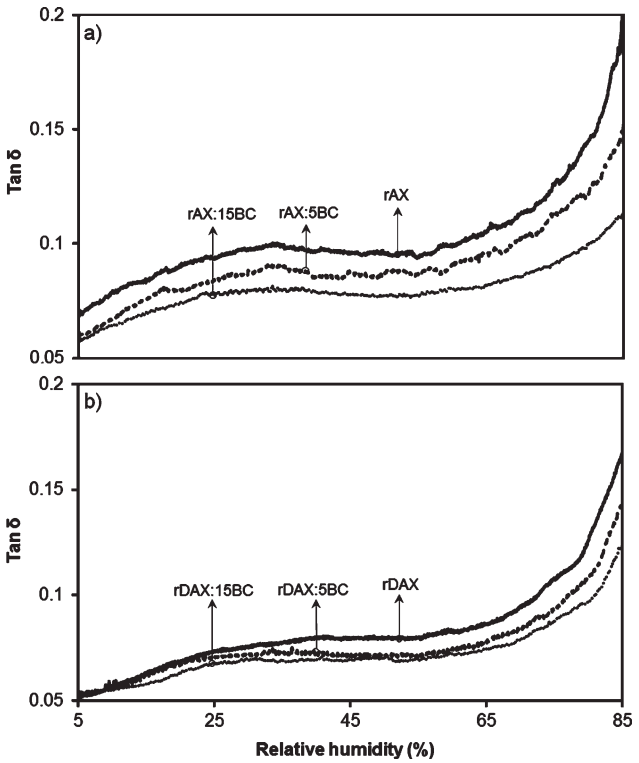

Figure 8 Tan δ of composite films as a function of relative humidity, showing their damping behavior; (a) rAX and (b) rDAX.

The loss tangent (tan δ) for the films increased, as expected, with an increasing RH (Fig. 8). Two transition points could be noted, a secondary transition around 20% RH and the main transition[24] at around 80% RH. The secondary transition was more apparent for the films (neat and composites) made from the unmodified arabinoxylan, rAX, and can be attributed to the arabinose substituents as being more apparent in the unmodified polymer. A higher amount of substituents will prevent intermolecular hydrogen bonding between xylan backbone and result in higher flexibility of the molecule.[25] This may result in an increased hydration and be seen as a clear plasticizing effect. The lower damping seen for the rDAX compared to the rAX film can be caused by the occurred crystallization, after debranching of the arabinose substituents.[26] The main transition at 80% RH was attributed to the moisture-induced glass transition of the arabinoxylan backbone.[27–29] Figure 8 also illustrates that the composite films showed a lower damping factor than the pure films; the higher the amount of the BC the lower the damping factor. Apart from the lowering due to the lower content of the xylan, also the possible interactions between cellulose and xylan might limit the moisture-induced mobility of the arabinoxylan chains.[7]

CONCLUSIONS

This work has demonstrated that it is possible to produce xylan films with improved strength properties with the addition of BC. Mixing of BC with xylans in a high-pressure microfluidiser resulted in optically transparent nanocomposite films.

With the reduction of the arabinosyl substituents of the xylan, from Ara/Xyl ratios of 0.50 to 0.16, moisture sensitivity, but only at very high relative humidities, was decreased, presumably due to some degree of xylan crystallization (20%). This also resulted in films of lower strength and breaking strain, that is, in more brittle films.

In general, stronger and stiffer films were produced when BC was added to the xylans. The addition of BC had though only marginal effects on the T_g of the xylan as well as of the moisture sorption ability. However, the reinforcement brought about quite noticeable reductions of the moisture sensitivity of the mechanical properties; a lower modulus decrease and a lower mechanical damping.

Formas, the Academy of Finland, and INRA are gratefully acknowledged for funding through the WoodWisdom-Net program. Wallenberg Wood Science Center is acknowledged for funding Guillermo Toriz and Paul Gatenholm. Novozymes A/S is acknowledged for supplying the α-L-arabinofuranosidase. The authors thank Anders Mårtensson for providing the SEM micrographs, Åsa Blademo for performing the homogenization, Susanna Heikkinen for help in rDAX preparation, and Miguel Pernes for performing the DEA and water sorption measurements.

References

1. Nisperos-Carriedo, M. O. In Edible Coatings and Films to Improve Food Quality; Krochta, J. M., Baldwin, E. A., Nisperos-Carriedo, M. O., Eds.; Technomic Publishing Company: Lancaster, 1994; Chapter 11.
2. Gröndahl, M.; Eriksson, L.; Gatenholm, P. Biomacromolecules 2004, 5, 1528.
3. Höije, A.; Sternemalm, E.; Heikkinen, S.; Tenkanen, M.; Gatenholm, P. Biomacromolecules 2008, 9, 2042.
4. Mikkonen, S. K.; Heikkinen, S.; Soovre, A.; Peura, M.; Serimaa, R.; Talja, A. R.; Helén, H.; Hyvönen, L.; Tenkanen, M. J Appl Polym Sci 2009, 114, 457.
5. Aspinall, G. O.; Sturgeon, R. J. J Chem Soc 1957, 4469.
6. Timell, T. E. Adv Carbohydr Chem Biochem 1964, 19, 247.
7. Ishii, T.; Shimizu, K. In Wood and Cellulosic Chemistry; Hon, D. N.-S., Shiraishi, N., Eds.; Marcel Dekker: New York, 2001; Chapter 5.
8. Bacic, A.; Harris, P. J.; Stone, B. A. In The Biochemistry of Plants; Preiss, J., Ed. Academic Press: New York, 1988; Chapter 8.
9. Brown, R. M. Jr.; Haigler, C. H.; Suttie, J.; White, A. R.; Roberts, E.; Smith, C.; Itoh, T.; Cooper, K. J Appl Polym Sci: Appl Polym Symp 1983, 37, 33.
10. Dammström, S.; Gatenholm, P. In Characterisation of the Cellulosic Cell Wall; Stokke, D. D., Groom, L. H., Eds.; Blackwell: Ames, 2006; Chapter 5.
11. Pitkänen, L.; Virkki, L.; Tenkanen, M.; Tuomainen, P. Biomacromolecules 2009, 10, 1962.

12. Poutanen, K. J Biotechnol 1988, 7, 271.
13. Matsuoka, M.; Tsuchida, T.; Matsushita, K.; Adachi, O.; Yoshinaga, F. Biosci Biotechnol Biochem 1996, 60, 575.
14. Dammström, S.; Salmén, L.; Gatenholm, P. Polymer 2005, 46, 10364.
15. Nieduszynski, I. A.; Marchessault, R. H. Biopolymers 1972, 11, 1335.
16. Kraus, W.; Nolze, G. J. J Appl Cryst 1996, 29, 301.
17. Guinier, A. X-ray Diffraction in Crystals, Imperfect Crystals, and Amorphous Bodies; Dover: New York, 1994; Chapter 5.
18. Dervilly-Pinel, G.; Tran, V.; Saulnier, L. Carbohydr Polym 2004, 55, 171.
19. Carpita, N.; McCann, M. In Biochemistry and Molecular Biology of Plants; Buchanan, B., Gruissem, W., Jones, R., Eds.; American Society of Plant Physiologists: Rockville, 2000; Chapter 2.
20. Marchessault, R. H.; Liang, C. Y. J Polym Sci 1962, 59, 357.
21. Marchessault, R. H. In Procidings of Symposium International sur la Chimie et la Biochimie de la Lignine, de la Cellulose et des Hemicelluloses; Chambéry, L. I. R.d., Ed.; Université de Grenoble: Grenoble, 1964.
22. Bishop, C. T. Can J Chem 1953, 31, 793.
23. Sternemalm, E.; Höije, A.; Gatenholm, P. Carbohydr Res 2008, 343, 753.
24. St-Germain, F. G. T.; Gray, D. G. J Wood Chem Technol 1987, 7, 33.
25. Almond, A.; Sheehan, J. K. Glycobiology 2003, 13, 255.
26. Andrewartha, K. A.; Phillips, D. R.; Stone, B. A. Carbohydr Res 1979, 77, 191.
27. Levine, H.; Slade, L. In Water Science Reviews; Franks, F., Ed.; Cambridge University Press: Cambridge, 1988; Chapter 2.
28. Olsson, A.-M.; Salmén, L. In Proceedings of the International Conference of COST Action E8. Mechanical Performance of Wood and Wood Products. Wood-Water Relation; Hoffmeyer, P., Ed.; Technical University of Denmark: Copenhagen, 1997.
29. Olsson, A.-M.; Salmén, L. In Proceedings of the ACS Symp Series 864 Hemicelluloses: Science and Technology; Gatenholm, P., Tenkanen, M., Eds.; American Chemical Society: Washington, 2004.